Biochemistry

 Volume 42, Number 8 March 4, 2003

New Concepts

Mechanistic Considerations for General Acid−Base Catalysis by RNA: Revisiting the Mechanism of the Hairpin Ribozyme†

Philip C. Bevilacqua*

Department of Chemistry, The Pennsylvania State University, University Park, Pennsylvania 16802

Received December 2, 2002; Revised Manuscript Received January 15, 2003

ABSTRACT: Several small ribozymes carry out self-cleavage at a specific phosphodiester bond to yield 2′,3′-cyclic phosphate and 5′-hydroxyl termini. Prior mechanistic and structural studies on the HDV ribozymes led to the proposal that the pK_a of C75 is shifted toward neutrality, making it an effective general acid. Recent mechanistic studies on the hairpin ribozyme have led to models in which protonation of G8 is required for phosphodiester cleavage, either for general acid catalysis or for electrostatic stabilization. Inspection of recent crystal structures of the hairpin ribozyme, including a complex with a vanadate transition state mimic, suggests an alternative model involving general acid−base catalysis with G8 serving as the general base and A38 as the general acid. This model is consistent with the literature on the hairpin ribozyme, including pH−rate profiles of wild-type and mutant ribozymes and solvent isotope effects. General mechanistic considerations for RNA catalysis suggest that the penalty for having general acids and bases with pK_as removed from neutrality is not as severe as expected. These considerations suggest that general acid−base catalysis may be a common mechanistic strategy of RNA enzymes.

Protein and RNA enzymes use a variety of mechanistic strategies to increase the rate and specificity of chemical reactions, including metal ion catalysis, strain, desolvation, positioning, and general acid−base catalysis (for reviews, see refs *1*−*3*). Among these, general acid−base catalysis, in which enzyme functional groups donate and accept protons, is one of the most common; for example, a survey of enzyme-catalyzed mechanisms reveals that the vast majority involve proton transfers to and from amino acid side chains (*4*). General acid−base catalysis allows stabilization of unfavorable charges that develop in the transition state. General acid−base catalysis also facilitates the activation of weak nucleophiles and the stabilization of poor leaving groups. Enzymes are thought to be better suited for proton transfer than water or buffer because they have functional groups positioned near the nucleophile and leaving group, and because these functional groups typically have pK_as near neutrality. For example, studies on the mechanism of RNase A supported a concerted reaction mechanism, consistent with the simultaneous optimal positioning of both the general acid and general base (*5*−*7*). Recent studies indicate that divalent metal ions, Mg^{2+} in particular, are catalytically nonessential in the mechanisms of small ribozymes, and make at most a 10−20-fold contribution to rate acceleration (*8*−*14*). This suggests that in many cases ribozymes may rely on catalysis by the nucleobases themselves, possibly involving general acid−base catalysis.

Effective general acid−base catalysis, it has been argued, requires atoms with pK_as near the pH of the reaction, which in the case of biology is ≈7.4. Since a general acid is

† Supported in part by a Camille Dreyfus Teacher-Scholar Award and a Sloan Fellowship.

* To whom correspondence should be addressed. E-mail: pcb@chem.psu.edu. Phone: (814) 863-3812. Fax: (814) 863−8403.

10.1021/bi027273m CCC: $25.00
Published on Web 02/07/2003

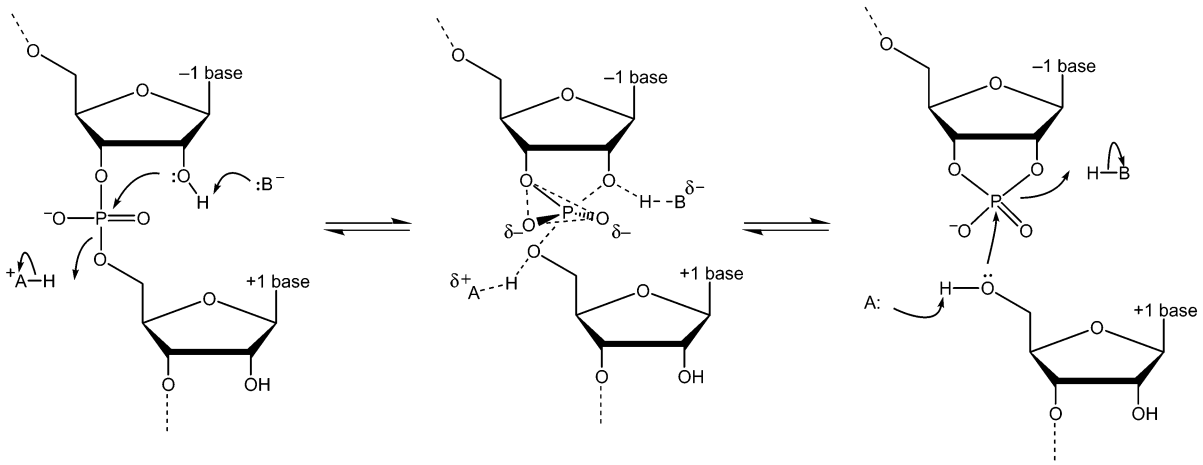

FIGURE 1: Mechanism for phosphodiester cleavage (forward direction) and ligation (reverse direction), with the transition state for a concerted reaction shown between them. Note that the general acid for the forward direction is the general base for the reverse direction. General acid−base catalysis can be seen to stabilize the transition state by redistributing charge from the attacking and leaving phosphoryl oxygens to the general acid and base. The functional forms of A and B for the forward direction are thought to be as follows: C75 $N3^+$ and $[Mg(H_2O)_5(OH)]^+$ for the HDV ribozyme, respectively, A38 $N1^+$ and G8 $N1^-$ for the hairpin ribozyme, respectively, and $His119^+$ and His12 for RNase A, respectively.

functional only when it has a proton *to* transfer, a very strong acid (with a pK_a of ≪7) is an ineffective general acid since it is primarily in the nonfunctional deprotonated form at neutral pH. Likewise, a very weak acid, while in the functional protonated form at neutral pH, is an ineffective general acid since it is reluctant to transfer its proton. Thus, the compromise is to have a pK_a near neutrality.[1] While this argument is generally valid, it is important to recognize that the actual contribution of a general acid or base to rate acceleration also depends on the Brønsted α and β values for the transition state. Since these are typically near 0.5 (rather than 0), the functional consequences of nonoptimal pK_as are lessened (see below).

In this article, the importance of general acid−base catalysis to rate acceleration of phosphodiester bond cleavage by the hairpin and HDV ribozymes[2] is considered in some detail. The identities of the putative general acid and base are derived from the positioning of atoms in crystal structures, as well as from functional studies. The principle of kinetic ambiguity and the influence of the Brønsted α and β values on the contribution of general acid−base catalysis are considered. It is concluded that general acid−base catalysis can make large contributions to rate acceleration even for nucleobases with pK_as of 5 and 9, and is therefore likely to be an important feature of the mechanisms of the HDV and hairpin ribozymes, as well as the ribosome.

Possibilities for General Acid−Base Catalysis Suggested by Ribozyme Crystal Structures

Several crystal structures have been determined for the HDV and hairpin ribozymes. The crystal structure of the self-cleaved form of the genomic HDV ribozyme revealed the possibility for general acid catalysis by C75 (*15*, *16*).[3] N3 of C75 was found to be within hydrogen bonding distance of the 5′-OH group of G1, and a C75A change had a ΔpK_a consistent with proton transfer from the imino nitrogen (Figure 1) (*17*, *18*). This suggested that N3 of C75 might be protonated in the precursor state of the ribozyme and serve as the general acid in the cleavage reaction (*14*, *18*).[4]

Rupert and co-workers have determined the crystal structure of the hairpin ribozyme in three different states: a precursor complex, a product complex, and a transition state complex in which vanadate was used to mimic the trigonal bipyramidal transition state (*20*, *21*). Comparison of these structures led the authors to conclude that the ribozyme binds the transition state more tightly than the precursor or the product, in an illustration of Pauling's postulate for enzyme catalysis.

In the precursor structure, which has a 2′-methoxy at the −1 position, G8 N1 is observed to donate a hydrogen bond to the 2′-oxygen of the methoxy group (*21*). In addition, the N6 amine of G8 appears to donate a hydrogen bond to a nonbridging oxygen of the scissile phosphate. In the transition state mimic structure, G8 N1 was found to donate a hydrogen bond to the 2′-bridging oxygen of the trigonal bipyramidal vanadate, while G8 N6 maintains the same interaction. In the product structure, G8 N1 is still protonated and donates a hydrogen bond to the 2′-bridging oxygen of the 2′,3′-cyclic phosphate. Thus, one interpretation is that G8 N1 remains protonated throughout the reaction and stabilizes the reaction by hydrogen bonding to the reactive phosphate and sugar. These interactions could be mediated by the G8 N1 imino proton or perhaps by protonation elsewhere on guanine, one possibility being N3 on the minor

[1] Similar arguments hold for general base catalysis, and lead to the conclusion that a pK_a near neutrality is optimal here as well.

[2] The hammerhead ribozyme also catalyzes a reaction that produces the same termini. However, a crystal structure clearly representing the active conformation is not available, and so is not discussed here.

[3] The HDV ribozyme also has a closely related antigenomic sequence, in which the C75 counterpart is C76. This residue is termed C75 here.

[4] It is important to distinguish between the forward and reverse directions of the reaction. On the basis of the principle of microscopic reversibility, the general acid for the forward direction serves as the general base for the reverse direction (see Figure 1). For the hairpin and HDV ribozymes, the *cleavage* reaction is termed the *forward* reaction here and the *ligation* reaction the *reverse* reaction; note that ligation has not been observed for the HDV ribozyme, presumably because it does not have a guide sequence to bind the leaving nucleotides (*19*).

Scheme 1

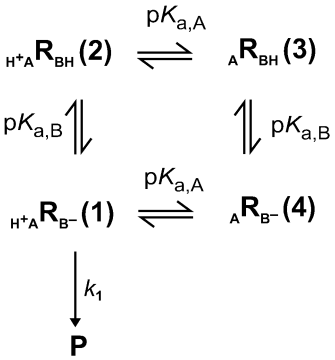

groove face (*22*). It has been suggested that water might then serve to deprotonate the 2′-hydroxyl at nucleotide −1 (*21*). This model is supported by kinetics experiments, which can be interpreted as being consistent with protonation of G8 required for cleavage (*22*, *23*).

However, these data are also consistent with an alternative mechanism in which a deprotonated N1 atom of G8 accepts a proton from the nucleophilic 2′-hydroxyl group in the cleavage reaction. Such an interaction is not possible in the precursor crystal since a 2′-methoxy is incapable of donating a hydrogen bond. This mechanism appears to be reasonable since G8 N1 donates a hydrogen bond to the 2′-bridging oxygen of the 2′,3′-cyclic phosphate product structure, suggesting it could serve as a general acid for ligation, and by microscopic reversibility as the general base for cleavage. This possibility is supported by pH−rate profiles as well (see the next section).

In a similar fashion, A38 N1 accepts a proton from the 5′-OH group of G1 in the product structure, positioning it to serve as the general base for the ligation reaction and as the general acid for the cleavage reaction. The positioning of A38 N1 in the hairpin ribozyme and that of C75 N3 in the genomic HDV ribozyme are strikingly similar, suggesting that these atoms may serve parallel mechanistic roles. In addition, both nucleobases utilize the adjacent amino group to hydrogen bond to a nearby phosphate, which may help shift the pK_as of the bases (see below). The possibility for general acid−base catalysis by A38 and G8 was raised by Rupert and co-workers (*20*, *21*). One goal of this article is to try to reconcile general acid−base catalysis with functional studies on the hairpin ribozyme and to suggest experiments to test the model further.

Qualitative Expectations: Shape of pH−Rate Profiles and the Principle of Kinetic Ambiguity

Before the experimental data available for the ribozymes are discussed, it is instructive to consider several mechanistic expectations. Scheme 1 shows a simple kinetic model in which a single general acid of the functional form HA^+, and a single general base of the functional form B^-, are involved in the reaction.[5] Protons can bind to A or B^- with pK_as of the conjugate acids, pK_{a,A^+} and p$K_{a,B}$, respectively, and it is assumed that the two protons do not influence each other.[6] In addition, it is assumed that of the four ribozyme states, only R(1), in which both the acid and base are in their functional forms, is capable of reacting to give products P, with a first-order rate constant k_1.[7]

Using this model, the partition function can be written as

$$Q = 1 + 10^{pK_{a,B}-pH} + 10^{pK_{a,B}-pK_{a,A}} + 10^{pH-pK_{a,A}} \quad (1)$$

This leads to the following expressions for the fraction, *f*, of each species

$$f_{HA^+} = \frac{1 + 10^{pK_{a,B}-pH}}{Q} \quad (2)$$

$$f_{B^-} = \frac{1 + 10^{pH-pK_{a,A}}}{Q} \quad (3)$$

$$f_{HA^+} f_{B^-} = \frac{1}{Q} = f_{R(1)} \quad (4)$$

In general, the log values of eqs 2−4 are plotted since this allows log $f_{R(1)}$ to be constructed from the sum of log f_{HA^+} and log f_{B^-}. Last, the rate constant observed in an experiment, k_{obs}, is simply the product of $f_{R(1)}$ and k_1

$$k_{obs} = f_{R(1)} k_1 \quad (5)$$

which leads to the equation

$$\log k_{obs} = \log f_{HA^+} + \log f_{B^-} + \log k_1 \quad (6)$$

Note that both f_{HA^+} and f_{B^-} are functions of pH, whereas k_1 is not; on the other hand, k_1 represents a bond-breaking event and is a function of Brønsted values α and β, whereas f_{HA^+} and f_{B^-} are not. The separation of variables in eq 6 allows pH effects, which shift the population distribution among the four ribozyme states, and transition state effects, which change the intrinsic reactivity of R(1), to be considered separately. In this section, the effects of the pK_a values of the general acid and base on the shapes of pH−rate profiles are considered for select cases, and the effects of the pK_a values on the magnitude of k_1 are considered in the next section.

In case 1, pK_{a,HA^+} = 6.2 and pK_{a,HB^+} = 5.8. This is the case for RNase A, which has pK_as for the its general acid, His119, and general base, His12, of 6.2 and 5.8, respectively (*24*). The logarithmic species plots for the functional forms of the acid and base are shown in Figure 2A, and their sum gives the log $f_{R(1)}$. The plot of log $f_{R(1)}$ versus pH gives the classic bell-shaped pH−rate profile. The slopes of the low- and high-pH regimes are 1 and −1, respectively, as expected for transfer of one proton. This case is understood to be near-optimal, since the two pK_as are close to neutrality. This is

[5] Whether the protonated form of the general acid or base is positively charged will depend on the case being considered, and will be pointed out for each case.

[6] This assumption may not always hold since the acid and base must be close to each other to catalyze the reaction; see, for example, the anticooperative interaction of C75 H^+ and $[Mg(H_2O)_5(OH^-)]^+$ in the HDV ribozyme (*18*). In the case of hairpin ribozyme self-cleavage, if the functional form of A38 is cationic and the functional form of G8 is anionic, positive cooperativity may result, leading to pK_a shifting toward neutrality and further favoring general acid−base catalysis. Any interaction can be modeled by multiplying the appropriate K_as by a cooperativity factor ω which does not change the general behavior described herein.

[7] This should be true if the reaction is concerted. More complex behavior arises when the general base switches during the reaction, although this can be treated with more complex kinetic models (*14*).

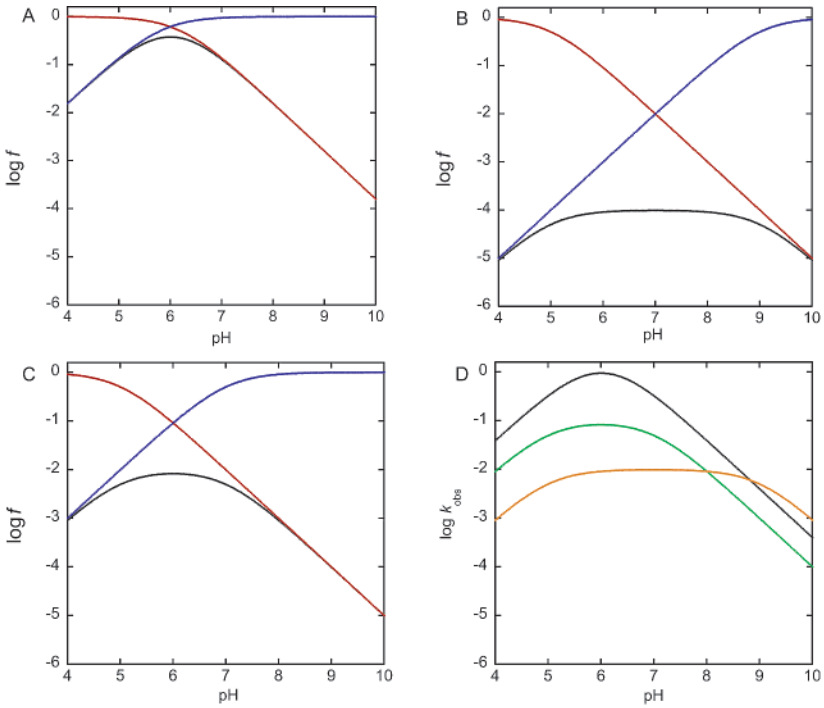

FIGURE 2: Simulations of pH−species plots and pH−k_{obs} profiles according to the kinetic model for general acid−base catalysis in Scheme 1. In panels A−C, the log of the fraction of the functional form of the acid, log f_{HA^+}, is given in red, the log of the fraction of the functional form of the base, log f_{B^-}, is given in blue, and the log of the fraction of ribozyme in the active state, log $f_{R(1)}$, is given in black. According to eq 4, log $f_{R(1)}$ = log f_{HA^+} + log f_{B^-}, which can be seen graphically. (A) For case 1, pH−species simulation using pK_a values for RNase A (pK_{a,HA^+} = 6.2 and pK_{a,HB^+} = 5.8) where the general acid and base are His119$^+$ and His12, respectively (*24*). (B) For case 2, pH−species simulation using pK_a values for wild-type hairpin ribozyme self-cleavage (pK_{a,HA^+} = 5.0 and p$K_{a,HB}$ = 9.0) (*23*), where the general acid and base are presumed to be A38$^+$ and G8$^-$, respectively. (C) For case 3, pH−species simulation using pK_a values for hairpin ribozyme self-cleavage with G8 diAP substitution (pK_{a,HA^+} = 5.0 and pK_{a,HB^+} = 7.0) (*23*). (D) pH−rate simulations of each case. Case 1 is black, case 2 orange, and case 3 green. According to eq 5, log k_{obs} = log k_1 + log $f_{R(1)}$, where log k_1 is a constant calculated as described in the text, and log $f_{R(1)}$ is from panels A−C.

manifested in the maximum log $f_{R(1)}$ value of approximately −0.43 ([R(1)$_{max}$] ≈ 37% × [R$_{total}$]), which occurs at pH 6.0. For this case, the pK_a at higher pHs is pK_{a,HA^+}, while that at lower pHs is pK_{a,HB^+}.

In case 2, pK_{a,HA^+} = 5 and p$K_{a,HB}$ = 9. This is the case considered here for the hairpin ribozyme, in which the general acid and base for the cleavage reaction are protonated A38 N1 and deprotonated G8 N1, respectively.[8,9] Figure 2B shows logarithmic species plots for this case. The plot for log f_{HA^+} levels off at pH values of less than ≈5, while that for log f_{B^-} levels off at pH values of greater than ≈9. Importantly, the plot for log $f_{R(1)}$ is nearly independent of pH between pH 5 and 9, which is the range over which most hairpin ribozyme experiments are conducted. This model is consistent with the known largely pH-independent behavior of the hairpin ribozyme reaction (*9*, *23*). According to this model, the observed pH independence is not because of an absence of protonation events on the ribozyme, but it is due instead to the decrease in the level of the functional form of the acid being offset by the increase in the functional form of the base. Note that at pH values of less than 5 and greater than 9, the bell-shaped pH−rate profile is recovered, and experiments down to pH 4.5 on the wild-type ribozyme are consistent with this idea.[8] Fedor raised this mechanistic possibility earlier, and argued that the pH independence is not because chemistry is not rate-limiting (*27*). Results for case 3 further support chemistry as the rate-limiting step.

This case is understood to be suboptimal since the two pK_as are removed from neutrality by 2 units each. This is manifested in the maximum log $f_{R(1)}$ value of approximately −3.99 ([R(1)$_{max}$] ≈ 0.01%[R$_{total}$]), which occurs between pH 6 and 8.[10] It should be noted, however, that the effect of

[8] The unperturbed pK_a for N1 of guanosine is near 9.4, and that for N1 of adenosine is near 3.5 (*25*). The value of 5 used for A38 is based in part on the pH−rate profiles for the wild-type hairpin ribozyme, which show a log linear decrease in rate below pH ≈5.5 (*23*). It has been noted that the effect near pH 5.5 can be suppressed somewhat with 50 mM Mg^{2+} (*23*), however high Mg^{2+} could shift the pK_a of A38 lower due to anticooperative effects. It is also possible that G8 may occupy alternative tauotomeric states that would affect the pK_a of N1 (*23*).

[9] This model is consistent with the crystal structures of Rupert and co-workers (*20*, *21*), but contradicts the model of Ryder et al., in which A38 was specifically implicated as *not* being the general base for the ligation reaction (*26*). These conclusions were based upon the absence of interference by an 8-azaadenosine analogue (unperturbed pK_a = 2.2) at A38. However, this pK_a is only 1.3 units lower than that for adenosine, and since A38 is implicated as the general base in the ligation reaction, this change would not have affected the fraction of A38 in the functional deprotonated form. The change would be predicted to decrease the rate, but only by $10^{\beta\Delta pK_a} = 10^{0.5(3.5-2.2)} = 4.5$-fold (see below for equation) at pH 5.5 and 6.5. In addition, a partial interference by 8-azaadenosine was found in a four-helix junction hairpin ribozyme (*26*).

[10] For Scheme 1, log $f_{R(1)}$ versus pH for the *ligation* reaction would be identical to that for the cleavage reaction. In this case, the plots of log f_{HA^+} would level off at pH values below ≈9, while that for log f_{B^-} would level off at pH values above ≈5. Although this $f_{R(1)}$ would be much larger than that for the forward reaction, this would be offset by the considerably lower intrinsic reactivity of neutral A38 and G8.

these suboptimal pK_a values on k_{obs} is not as severe as suggested by consideration of $f_{R(1)}$ alone (see the next section).

For case 3, p$K_{a,HA^+} = 5$ and p$K_{a,HB^+} = 7$. This is the case proposed for the hairpin ribozyme, in which G8 is substituted with a nucleobase having a pK_a closer to neutrality, such as 2,6-diaminopurine (diAP). Modeling of this reaction according to Scheme 1 leads to a log f_B plot that levels off at pH values above ≈7 (Figure 2C). The plot of log $f_{R(1)}$ versus pH now comes close to approximating the classical bell-shaped pH−rate profile of RNase A, and is very similar to profiles reported for this hairpin mutant (*22*, *23*). It is important to note that according to this model, the decrease in rate above pH 7 is because of a loss in the functional form of the general acid at position 38 rather than a requirement for protonation at position 8. Since changes at an active site residue lead to changes in the pH−rate profile, it is likely that the pH−rate profile arises from pH effects on catalysis rather than on structure.

There is, however, a kinetically equivalent mechanism that must be considered. It is possible that there is no general acid−base catalysis and that the protonated state of A38 is unimportant in the reaction. In this scenario, the decrease in rate above pH 7 would be ascribed to a loss in the level of the protonated form of position 8, meaning that the protonated form of the nucleobase at position 8 is important for the reaction. This is the model favored in several recent reports on the hairpin ribozyme (*22*, *23*), and is the opposite of that offered in the simulations in panels B and C of Figure 2. The ability of two opposing mechanisms to explain the data is what Jencks terms the "principle of kinetic ambiguity" (*28*). The question then is, "How can one distinguish between these two kinetically equivalent possibilities?" Multiple approaches are possible, and applying several of these at once can serve to strengthen support for a specific kinetic model.

(1) Crystal structures can give guidance, as only one model is generally consistent with the crystal structure. (2) In the case of the hairpin ribozyme, if a cationic form of position 8 were important, perhaps to act as an oxyanion hole, then diAP would be predicted to be a much better reagent than guanine at pH values below ≈6, since diAP is positively charged at these pH values and guanine is not. However, G is approximately 10-fold faster than diAP at position 8 (*23*), suggesting that positive charge at position 8 is unimportant. (3) In the case of RNase A, the leaving group in the reaction was changed to an exceptionally good one, *p*-nitrophenol. It was shown that His119 makes a very small contribution to rate for this substrate, implicating His119 in protonating the leaving group oxygen when a poor leaving group is present (*6*). (4) In the case of the HDV ribozyme, negative linkage was observed for binding of a proton and a Mg^{2+} ion to the ribozyme (*18*), implicating C75 as a protonated species. In addition, omission of Mg^{2+} led to inversion of the observed pH−rate profile (*14*, *18*), although the role of C75 is not entirely clear in the absence of Mg^{2+} because of the involvement of protonated C41 in the pH−rate profile (*29*).

Quantitative Expectations: Magnitude of the Penalty for Nonoptimal pK_as

The cases considered above suggest that general acid−base catalysis might be operational even if the pK_as of the general acid and base are not at neutrality. This leads to the question, "How penalizing are pK_as removed from neutrality?" The kinetic model in Scheme 1 led to eq 6, which indicates that the contributions of f_{HA^+}, f_{B^-}, and k_1 to the observed rate constant, k_{obs}, can be treated separately. As mentioned, k_1 is a first-order rate constant for R(1) and is therefore not a direct function of pH. In general, k_1 will be larger the lower the pK_a of the general acid and the higher the pK_a of the general base. The rate constants for protonation, k_{HA^+}, and deprotonation, k_{B^-}, are given by the Brønsted equations

$$\log k_{HA^+} = -\alpha(pK_{a,HA^+}) + \log G_A \quad (7)$$

$$\log k_{B^-} = \beta(pK_{a,HB}) + \log G_B \quad (8)$$

where G_A and G_B are constants for a given reaction and α and β describe the degree of proton transfer in the transition state, with possible values between 0 and 1 (*28*); values of α and β for proton transfer for phosphodiester bond cleavage are near 0.5, and are supported by studies on the HDV ribozyme (*14*, *30*) and RNase A (*6*). To apply the Brønsted equations to k_{obs} in Scheme 1, the concerted reaction was modeled as two proton reactions in series. If pK_{a,HA^+} and p$K_{a,HB}$ are equally removed from neutrality (e.g., pK_{a,HA^+} = 5 and p$K_{a,HB} = 9$), then it is assumed that $k_1 \approx k_{HA^+} \approx k_{B^-}$. However, if one of the pK_as is further removed from neutrality than the other (e.g., p$K_{a,HA^+} = 5$ and p$K_{a,HB} = 7$), then k_1 is assumed to be dominated by the weaker species, in this case k_{B^-}. k_1 for case 2 (Figure 2B) was arbitrarily set to 100, providing a log k_1 contribution of 2 to the log k_{obs} summation (eq 6). The value of log k_1 for case 1 (Figure 2A) was calculated to be 0.4 [from $k_1/100 = 10^{\beta(\Delta pK_{a,bases})} = 10^{0.5(5.8-9)}$], and log k_1 for case 3 was calculated to be 1 [from $k_1/100 = 10^{\beta(\Delta pK_{a,bases})} = 10^{0.5(7-9)}$].

The calculated pH−k_{obs} profiles are shown in Figure 2D. Addition of the k_1 term does not change the shapes of the curves; however, the curves approach each other more closely than the pH−$f_{R(1)}$ curves. In particular, at pH 6 case 2 (for the hairpin ribozyme) is only ≈200-fold slower than case 1 (for RNase A) (ratio of k_{obs}s is $0.97/5.0 \times 10^{-3}$). At a biological pH of 7.4, these two cases are even more similar, with case 2 being only ≈14-fold slower than case 1 (k_{obs}s = $0.14/1.0 \times 10^{-2}$). This illustration serves to show that the penalty for nonoptimal pK_a values is not as great as might be expected; protonated adenine and deprotonated guanine are a better acid and base than protonated and deprotonated histidine, respectively, and RNase A is optimized for pH 6.0 rather than pH 7.4.

Another interesting comparison is between a nucleobase with an unshifted pK_a and 55 M water, asking which would make the larger contribution to rate acceleration as a general base. Since guanine is a candidate for a general base in the hairpin ribozyme mechanism, the effect of substituting a guanine general base with water, which would go from H_2O to H_3O^+, will be made. Assuming that water is present near the nucleophilic 2′-hydroxyl at the same effective concentration as guanine, one can estimate the effect on k_{obs}. Using the relationship $k_1/100 = 10^{\beta(\Delta pK_{a,bases})} = 10^{0.5(-1.7-9)}$ provides a log k_1 of −3.35 for water, which is much smaller than the log k_1 of 2 for deprotonated guanine. Since essentially all of the water would be in the correct functional form to accept

a proton, log f_B would be 0, which is considerably larger than the log f_{B^-} of −2 for guanine. If it is assumed that other than the difference of water acting as the general base, the ribozyme was reacting according to case 2 (Figure 2B), then log $k_{obs}(H_2O) = -5.35$ (=−2 + 0 − 3.35) (eq 6). Comparison to k_{obs} for case 2 with a deprotonated guanine general base (Figure 2D) gives a log k_{obs}(G) of −2 (=−2 + −2 + 2), which leads to the prediction that guanine with a pK_a of ≈9 will be ≈2200 times more reactive than water.[11] This comparison stresses the important contribution nucleobases with nonoptimal pK_as can make to catalysis.

pK_a Shifting: Comparisons of Local Environments

The discussion above assumed a pK_a value of 5 for A38 in the hairpin ribozyme.[8] The unperturbed pK_a for A38 is ≈3.5, indicating that the pK_a of A38 may be shifted upward by ≈2 units. Similar pK_a shifting has been observed for the HDV ribozyme, although in this case a cytosine (C75) is involved, and the shifting is from 4.2 to ≈6 at saturating Mg^{2+} (*17*, *18*). As discussed above, this would aid the contribution of general acid catalysis to the rate. It is curious that for both ribozymes it is the general acid and not the general base that has the pK_a shifted in the direction of neutrality. This suggests that stabilizing the developing charge on the 5′-bridging oxygen leaving group is particularly important, which is consistent with physical organic considerations for phosphodiester cleavage (*18*, *31*−*33*).

Common to adenine and cytosine is an exocyclic amino group adjacent to the imino nitrogen. Furthermore, in both cases the amine hydrogen bonds to a nearby phosphate, in the HDV ribozyme to the phosphate of C22 (*15*), and in the hairpin ribozyme to the scissile phosphate in the transition state mimic (*21*). Also, the amino group of A38 has been shown to be critical for the reaction (*26*). It is possible that amine−phosphate interaction hinders rotation of the exocyclic amine, allowing for greater electron donation into the aromatic ring which would delocalize the positive charge off the imino nitrogen and put part of it in the neighborhood of the negatively charged phosphate. Cooperative interactions between oppositely charged acid and base species may also be important.[6] NMR experiments on the HDV ribozyme suggest that extensive shifting of the pK_a of C75 does not occur in the ground state of the cleaved ribozyme (the largest shift observed was to 5.4) (*34*). Perhaps extensive stabilization of the positive charge occurs upon formation of the transition state, or in the precursor structure.

Comparisons of Proton Inventories

Proton inventory experiments have been carried out on the hairpin and HDV ribozymes, and on RNase A (*23*, *30*, *35*, *36*). In the proton inventory, k_{obs} is measured as a function of the atom fraction of D_2O in the solution. Graphical analysis of the resultant curves allows the number of protons "in flight" in the transition state of the rate-limiting step, or steps, to be estimated. In all three enzymes, proton inventories have been found that are consistent with two proton transfers in the rate-limiting step (*23*, *35*, *36*), although single proton inventories have also been found for the HDV ribozyme under certain solution conditions (*30*). These experiments suggest that under appropriate conditions RNA enzymes can utilize two proton transfers in phosphodiester cleavage in a fashion similar to that of protein enzymes, and emphasize the potential importance of general acid−base catalysis in facilitating these transfers.

Implications for RNA Catalysis on the Ribosome

It is interesting to consider how these principles might impact mechanistic understanding of peptide bond formation on the ribosome. Recent studies provided a pH−rate profile in which the rate increases with pH to ≈7.5, followed by a leveling off (*37*). This profile has been largely interpreted as reflecting the importance of general base catalysis in the mechanism (*37*−*39*). However, the pH−rate profile is equally consistent with a general acid with a pK_a of 7.5 working in concert with a general base that has a pK_a above ≈9, as pointed out by Green and Lorsch (*39*). [An identical pH−rate profile was seen for the HDV ribozyme and was consistent with these pK_a assignments (*14*, *18*).] The possible importance of protonated A2451 N3 as a general acid or an oxyanion hole is consistent with the crystal structure of the 50S subunit, and was suggested when it was determined (*40*); moreover, this atom appears to have a pK_a near 7.5, as determined by chemical modification (*41*). On the basis of the mechanisms of the HDV and hairpin ribozymes, protonation of the leaving alkoxide may be particularly important in the reaction mechanism.

Chamberlin and co-workers recently implicated the 2′-hydroxyl of the ribosome-bound P-site adenosine in stabilizing positive charge in the transition state of amide synthesis (*42*). Since the pK_a of the 2′-hydroxyl in RNA is estimated to be 14.9 (*43*), participation of a 2′-hydroxyl as a high-pK_a general base and A2451 as a general acid with a pK_a near 7 offers an alternative model that is consistent with the recent pH−rate data.

Summary and Perspective

In this paper, the shapes and magnitudes of pH−rate profile curves were analyzed which led to the notion that general acid−base catalysis occurs in the mechanisms of the HDV and hairpin ribozymes. pH−rate profiles allowed pK_a values to be discerned and two kinetically equivalent mechanisms to be written. Crystal structures of these ribozymes supported one of the two mechanisms. It was concluded that the penalty for nonoptimal pK_as is not as severe as expected, although shifting of the pK_a of the general acid toward neutrality appears to be important for stabilizing an alkoxide leaving group. These considerations suggest that general acid−base catalysis, which is an essential feature of most protein enzyme reactions, may be a common feature of ribozyme reaction mechanisms. In the future, distinguishing the mechanistic roles of specific nucleobases in ribozymes, including the ribosome, may require testing their importance in the presence of good leaving groups, as was done for RNase A (*6*). General acid−base catalysis greatly expands the variety of reactions RNA can catalyze, which would be expected to enhance its evolvability.

ACKNOWLEDGMENT

I thank the members of my lab for comments on the manuscript. I am also indebted to Professors Marty Bollinger,

[11] The penalty for deletion of G8 has been measured at 350-fold (*22*), which is in reasonable agreement with this estimate.

Squire Booker, Barbara Golden, and Juliette Lecomte for thoughtful comments on the manuscript.

REFERENCES

1. Jencks, W. P. (1975) *Adv. Enzymol. 43*, 219−410.
2. Fersht, A. (1985) *Enzyme Structure and Mechanism*, 2nd ed., Freeman, New York.
3. Narlikar, G. J., and Herschlag, D. (1997) *Annu. Rev. Biochem. 66*, 19−59.
4. Silverman, R. B. (2000) *The Organic Chemistry of Enzyme-Catalyzed Reactions*, Academic Press, San Diego.
5. Herschlag, D. (1994) *J. Am. Chem. Soc. 116*, 11631−11635.
6. Thompson, J. E., and Raines, R. T. (1994) *J. Am. Chem. Soc. 116*, 5467−5468.
7. Sowa, G. A., Hengge, A. C., and Cleland, W. W. (1997) *J. Am. Chem. Soc. 119*, 2319−2320.
8. Hampel, A., and Cowan, J. A. (1997) *Chem. Biol. 4*, 513−517.
9. Nesbitt, S., Hegg, L. A., and Fedor, M. J. (1997) *Chem. Biol. 4*, 619−630.
10. Young, K. J., Gill, F., and Grasby, J. A. (1997) *Nucleic Acids Res. 25*, 3760−3766.
11. Murray, J. B., Seyhan, A. A., Walter, N. G., Burke, J. M., and Scott, W. G. (1998) *Chem. Biol. 5*, 587−595.
12. Curtis, E. A., and Bartel, D. P. (2001) *RNA 7*, 546−552.
13. O'Rear, J. L., Wang, S., Feig, A. L., Beigelman, L., Uhlenbeck, O. C., and Herschlag, D. (2001) *RNA 7*, 537−545.
14. Nakano, S., Proctor, D. J., and Bevilacqua, P. C. (2001) *Biochemistry 40*, 12022−12038.
15. Ferre-D'Amare, A. R., Zhou, K., and Doudna, J. A. (1998) *Nature 395*, 567−574.
16. Ferre-D'Amare, A. R., and Doudna, J. A. (2000) *J. Mol. Biol. 295*, 541−556.
17. Perrotta, A. T., Shih, I., and Been, M. D. (1999) *Science 286*, 123−126.
18. Nakano, S., Chadalavada, D. M., and Bevilacqua, P. C. (2000) *Science 287*, 1493−1497.
19. Wadkins, T. S., and Been, M. D. (2002) *Cell. Mol. Life Sci. 59*, 112−125.
20. Rupert, P. B., and Ferre-D'Amare, A. R. (2001) *Nature 410*, 780−786.
21. Rupert, P. B., Massey, A. P., Sigurdsson, S. Th., and Ferre-D'Amare, A. R. (2002) *Science 298*, 1421−1424.
22. Lebruska, L. L., Kuzmine, II, and Fedor, M. J. (2002) *Chem. Biol. 9*, 465−473.
23. Pinard, R., Hampel, K. J., Heckman, J. E., Lambert, D., Chan, P. A., Major, F., and Burke, J. M. (2001) *EMBO J. 20*, 6434−6442.
24. Raines, R. T. (1998) *Chem. Rev. 98*, 1045−1065.
25. Saenger, W. (1984) *Principles of Nucleic Acid Structure*, Springer-Verlag, New York.
26. Ryder, S. P., Oyelere, A. K., Padilla, J. L., Klostermeier, D., Millar, D. P., and Strobel, S. A. (2001) *RNA 7*, 1454−1463.
27. Fedor, M. J. (2000) *J. Mol. Biol. 297*, 269−291.
28. Jencks, W. P. (1969) in *Catalysis in Chemistry and Enzymology*, Dover Publications Inc., New York.
29. Wadkins, T. S., Shih, I., Perrotta, A. T., and Been, M. D. (2001) *J. Mol. Biol. 305*, 1045−1055.
30. Shih, I. H., and Been, M. D. (2001) *Proc. Natl. Acad. Sci. U.S.A. 98*, 1489−1494.
31. Kirby, A. J., and Younas, M. (1970) *J. Chem. Soc. B*, 510−513.
32. Oivanen, M., Kuusela, S., and Lonnberg, H. (1998) *Chem. Rev. 98*, 961−990.
33. Herschlag, D., Eckstein, F., and Cech, T. R. (1993) *Biochemistry 32*, 8312−8321.
34. Luptak, A., Ferre-D'Amare, A. R., Zhou, K., Zilm, K. W., and Doudna, J. A. (2001) *J. Am. Chem. Soc. 123*, 8447−8452.
35. Matta, M. S., and Vo, D. T. (1986) *J. Am. Chem. Soc. 108*, 5316−5318.
36. Nakano, S., and Bevilacqua, P. C. (2001) *J. Am. Chem. Soc. 123*, 11333−11334.
37. Katunin, V. I., Muth, G. W., Strobel, S. A., Wintermeyer, W., and Rodnina, M. V. (2002) *Mol. Cell 10*, 339−346.
38. Hansen, J. L., Schmeing, T. M., Moore, P. B., and Steitz, T. A. (2002) *Proc. Natl. Acad. Sci. U.S.A. 99*, 11670−11675.
39. Green, R., and Lorsch, J. R. (2002) *Cell 110*, 665−668.
40. Nissen, P., Hansen, J., Ban, N., Moore, P. B., and Steitz, T. A. (2000) *Science 289*, 920−930.
41. Muth, G. W., Ortoleva-Donnelly, L., and Strobel, S. A. (2000) *Science 289*, 947−950.
42. Chamberlin, S. I., Merino, E. J., and Weeks, K. M. (2002) *Proc. Natl. Acad. Sci. U.S.A. 99*, 14688−14693.
43. Lyne, P. D., and Karplus, M. (2000) *J. Am. Chem. Soc. 122*, 166−167.

BI027273M